CERN-TH.6015/91
CPT-91/P.2416
FTUV/91-9

The $K^0 - \bar{K}^0$ B-factor in the QCD-hadronic duality approach

J.Prades [a], **C.A. Dominguez** [b], **J.A. Peñarrocha** [a], **A. Pich** [c] and **E. de Rafael** [c,d]

a) Departament de Física Teòrica and Institut de Física Corpuscular (CSIC), Universitat de València, E-46100 Burjassot, (València) Spain.
b) Institute of Theoretical Physics and Astrophysics, University of Cape Town, South Africa.
c) Theoretical Physics Division, CERN, CH-1211 Geneva 23, Switzerland.
d) Centre de Physique Théorique, Section 2, C.N.R.S.-Luminy, Case 907, F-13288 Marseille Cedex 9, France.

ABSTRACT

We report on an improved calculation of the B-parameter within the QCD-hadronic duality approach proposed in ref. [1]. Particular emphasis is given to details of the hadronic parametrization which is required to implement this approach. The result we find for the "invariant" B-parameter (see eqs. (1), (2) and (3) for definitions) is $\hat{B} = 0.39 \pm 0.10$.

CERN-TH.6015/91
CPT-91/P.2416
FTUV/91-9
February 1991

1 INTRODUCTION

The B-factor is a parametrization of the K^0 to $\bar{K}^0$ matrix element of the four-quark operator

$$\mathcal{O}_{\Delta S=2}(x) \equiv \bar{s}_\alpha(x)\gamma^\mu \left(\frac{1-\gamma_5}{2}\right) d^\alpha(x)\bar{s}_\beta(x)\gamma_\mu \left(\frac{1-\gamma_5}{2}\right) d^\beta(x), \qquad (1)$$

where α and β denote quark-colour indices. Conventionally it is defined by the relation

$$<\bar{K}^0|\mathcal{O}_{\Delta S=2}|K^0> \;=\; \frac{4}{3} f_K^2 M_K^2 B, \qquad (2)$$

where f_K denotes the $K \to \mu\nu$ coupling ($f_K = 119$ MeV) and M_K the K^0-mass. A reliable determination of this B-parameter would help very much to make progress in the phenomenological analysis of CP-violation within the framework of the Standard Model (SM).

Various approaches to calculate B and similar factors which parametrize other hadronic matrix elements of four-quark operators, have been discussed in the literature [1]-[9]. Here we shall be concerned with the method based on QCD-hadronic duality sum rules, which was already suggested some time ago [1]. The result found for the B-factor within this approach in ref. [1] is

$$|\hat{B}| \equiv |B|\,\alpha_s(\mu^2)^{-2/9} \;=\; 0.33 \pm 0.09. \qquad (3)$$

The μ-scale dependence of B reflects the fact that the four-quark operator $\mathcal{O}_{\Delta S=2}$ in (1) has an anomalous dimension. The error in (3) is an educated error guess mainly due to the dependence on the phenomenological parametrization of the various hadronic spectral functions which appear in the calculation. The main purpose of this paper is to report on an improved analysis of the hadronic parametrization which is required to implement this approach.

2 THE QCD-HADRONIC DUALITY APPROACH

The relevant quantity in this approach is the two-point function associated with the local four-quark operator $\mathcal{O}_{\Delta S=2}(x)$ in (1); *i.e.*, the function

$$\Psi(q^2) \;=\; i\int d^4x e^{iqx} <0|T(\mathcal{O}_{\Delta S=2}(x)\mathcal{O}^\dagger_{\Delta S=2}(0))|0>. \qquad (4)$$

Perturbative QCD predicts the behaviour of this function at short-distances; *i.e.*, large $-q^2 \equiv Q^2$ values. On the other hand, the absorptive part of this function

is a physical observable defined as the sum over hadronic on-shell states Γ with overall strangeness $S = 2$; *i.e.*,

$$\frac{1}{\pi}\, Im\, \Psi^{had}(t) \;=\; \sum_\Gamma <0|\mathcal{O}_{\Delta S=2}|\Gamma><\Gamma|\mathcal{O}^\dagger_{\Delta S=2}|0>. \qquad (5)$$

Implicit in the summation here is an integral over phase space and an energy-momentum conserving δ-function.

The analyticity properties of two-point functions relate integrals of the spectral function in (5) to quantities which are calculable via perturbative QCD. These are the so-called Finite Energy Sum Rules (FESR) [10]. In practice we shall need two of these sum rules:

$$F(s_0) \;=\; \int_{4M_K^2}^{s_0} dt\, \frac{1}{\pi}\, Im\, \Psi^{had}(t) \qquad (6)$$

and

$$G(s_0) \;=\; \int_{4M_K^2}^{s_0} dt\, t\, \frac{1}{\pi}\, Im\, \Psi^{had}(t). \qquad (7)$$

The lower threshold in these integrals corresponds to the K^0K^0 state, which is the lowest energy state with $S = 2$. The higher threshold s_0 is the onset of the asymptotic QCD continuum in the hadronic spectral function. The value of s_0 must be large enough so that

$$\frac{1}{\pi}\, Im\, \Psi^{had}(t) \approx \frac{1}{\pi}\, Im\, \Psi^{QCD}(t) \approx \frac{1}{(16\pi^2)^3}\, \frac{2}{15}\, t^4 \qquad \text{for } t \geq s_0. \qquad (8)$$

The functions F and G have been evaluated in perturbative QCD with the inclusion of α_s-corrections and finite strange quark mass corrections [1]. The effects of the leading $\frac{1}{s_0}$-power corrections due to the quark condensate $m_s<\bar{s}s>$ and the gluon condensate $<\frac{\alpha_s}{\pi} G^2>$ [11] have also been taken into account [1]. The explicit form of these functions is given in an appendix.

Of particular interest in this approach is the contribution to the hadronic spectral function $\frac{1}{\pi}\, Im\, \Psi^{had}(t)$ from the lowest K^0K^0 state. The matrix element $<0|\mathcal{O}_{\Delta S=2}|K^0K^0>$ that appears in (5) is precisely the crossed channel of the one in (2) which defines the B-factor. We propose to use the chiral realization of the four-quark operator $\mathcal{O}_{\Delta S=2}$ in terms of pseudoscalar particles to relate both matrix elements in a way which we discuss next.

To lowest order in the number of derivatives and using the definition

$$L_\mu \;=\; -\,i\,\frac{f_\pi^2}{2}\, U^\dagger \partial_\mu U \qquad (9)$$

where $U(x)$ is a flavour 3×3 matrix which incorporates the pseudoscalar fields ($UU^\dagger = 1$, $\det U = 1$, see ref. [17] for details),

$$\mathcal{O}_{\Delta S=2} \Rightarrow \frac{4}{3}\frac{f_K^2}{f_\pi^2} B\, L_\mu(x)_{23} L^\mu(x)_{23}. \qquad (10)$$

The overall normalization of this bosonic realization is not given by chiral symmetry requirements. The factors in (10) have been fixed so that with this definition of $\mathcal{O}_{\Delta S=2}$, the calculation of the $<\bar{K}^0|\mathcal{O}_{\Delta S=2}|K^0>$ matrix element reproduces the r.h.s. in (2). In other words, the B parameter here plays the rôle of an unknown coupling constant. The contribution to the hadronic spectral function from the K^0K^0 state induced by the operator in the r.h.s. of (10) can then be readily obtained with the result

$$\frac{1}{\pi}\, Im\, \Psi^{KK}(t) = \Theta(t-4M_K^2)\,|B|^2\,\frac{1}{16\,\pi^2}\,\frac{2}{9}\,f_K^4\,(t-2M_K^2)^2\,\sqrt{1-\frac{4M_K^2}{t}}. \qquad (11)$$

We now have the essential ingredients to explain the basic features of our approach to determine $|B|$. To a first very crude approximation, we shall choose as a parametrization of the hadronic spectral function the following *ansatz*

$$\frac{1}{\pi}\, Im\, \Psi^{had}(t) = \Theta(s_0-t)\,\frac{1}{\pi}\, Im\, \Psi^{KK}(t) + \Theta(t-s_0)\,\frac{1}{(16\,\pi^2)^3}\,\frac{2}{15}\,t^4\,\{1+\cdots\} \qquad (12)$$

with $\frac{1}{\pi}\, Im\, \Psi^{KK}(t)$ as given in (11), and where the second term in the r.h.s. is the leading QCD behaviour predicted by asymptotic freedom [1]. This parametrization is expected to be rather good at very low-t values, near the K^0K^0 threshold, and at very large-t values. It is very likely a gross misrepresentation of the physical behaviour at intermediate-t values where other hadronic channels contribute. Inserting the simple *ansatz* (12) in (6) we can then solve for $|B|$. The result, which obviously must depend on s_0, is shown in Fig. 1 where $|B|$ is plotted versus s_0 in GeV^2. The curve (0) in Fig. 1 shows the result found when we only use the leading behaviour of $F(s_0)$ as predicted by asymptotic freedom, *i.e.*; eq. (A.7a). Fig. 2 shows the corresponding result (the curve (0)) with use of the full expression for $F(s_0)$ in (A.6a). There is a nice minimum in the curve (0) in Fig. 1, which corresponds to the value $|B| \approx 1.5$. However, the s_0-value at this minimum ($s_0 \approx 1.9$ GeV^2) is too small to justify that the minimum in question is a signal of stability. The power corrections in $F(s_0)$ at such low-s_0 values are more than 100%. To improve on this result requires further input in the hadronic parametrization. This will push higher up the stability regime in s_0 to values where we can trust better the QCD calculation of the $F(s_0)$ function.

The next particle hadronic state which can contribute to the r.h.s. in (5) is the $\Gamma = KK\pi$ state. We use the same bosonic realization as in (10) to fix the low energy behaviour of this contribution as well as the overall normalization. However, contrary to the K^0K^0 state where no resonance with $S = 2$, $I = 1$ and $J = 0$ is known, the $KK\pi$ state can be in a $(K\pi)_{J=1,I=1/2}$ state which when combined with the K in an overall orbital angular momentum $l = 1$, gives us a $KK\pi$ state with $J = 0$. The $K\pi$ sub-state has a resonance, the $K^*(892)$, with $J^P = 1^-$, $I = 1/2$. In fact this possibility is already hinted by the quantum number structure of the bosonic realization in (10). With the parametrization

$$U(x) = \exp\left(-i\,\frac{\sqrt{2}}{f_\pi}\,\Phi(x)\right), \qquad (13)$$

where

$$\Phi(x) = \begin{pmatrix} \frac{\pi^0}{\sqrt{2}} + \frac{\eta}{\sqrt{6}} & \pi^+ & K^+ \\ \pi^- & -\frac{\pi^0}{\sqrt{2}} + \frac{\eta}{\sqrt{6}} & K^0 \\ K^- & \bar{K}^0 & -\frac{2\eta}{\sqrt{6}} \end{pmatrix}, \qquad (14)$$

and expanding L_μ in (9) in powers of Φ we find

$$L_\mu = -\frac{1}{\sqrt{2}}\,f_\pi\,\partial_\mu\Phi - \frac{i}{2}\,[\Phi,\partial_\mu\Phi] + \frac{1}{3\sqrt{2}}\,\frac{1}{f_\pi}\,[\Phi,[\Phi,\partial_\mu\Phi]] + \cdots, \qquad (15)$$

where the first term is a 0^- state, the second is a vector $\Phi\Phi$ state, the third an axial $\Phi\Phi\Phi$ state. The $(K\pi)$ $J^P = 1^-$ sub-state appears in the second term. We propose to insert the contribution from the $K\pi$ intermediate state in the hadronic spectral function as the one suggested by the chiral bosonic realization, but with a Breit-Wigner factor which modulates the chiral behaviour. More precisely, in a conventional chiral perturbation calculation, the expression for the $S = 1$, $J^P = 1^-$ spectral function is

$$\frac{1}{\pi}\, Im\, \Pi_V^{(1)}(t)_{\rm chiral} = \frac{1}{32\,\pi^2}\left(1-\frac{M_K^2}{t}\right)^3\,\Theta(t-M_K^2), \qquad (16)$$

where the pion mass has been neglected. Here, we propose to improve this spectral function via the replacement

$$\frac{1}{\pi}\, Im\, \Pi_V^{(1)}(t)_{\rm chiral} \Rightarrow \frac{1}{\pi}\, Im\, \Pi_V^{(1)}(t) = \frac{1}{\pi}\, Im\, \Pi_V^{(1)}(t)_{\rm chiral}\,|f_{K^*}(t)|^2 \qquad (17)$$

with $|f_{K^*}(t)|^2$ the square of a form factor which we simulate by the Breit-Wigner.

$$|f_{K^*}(t)|^2 = \frac{M_{K^*}^4 \left(1 + \frac{\Gamma_{K^*}^2}{M_{K^*}^2}\right)}{\left(t - M_{K^*}^2\right)^2 + M_{K^*}^2 \Gamma_{K^*}^2}, \tag{18}$$

where M_{K^*} is the mass and Γ_{K^*} the total width of the K^*-resonance. Notice that at $t = 0$ $|f_{K^*}(0)|^2 = 1$; *i.e.*, at low-t values the spectral function has the correct chiral behaviour.

With respect to the first K^0K^0-approximation we previously discussed, we propose now the improved *ansatz*

$$\begin{aligned}\frac{1}{\pi} Im\, \Psi^{had}(t) = \Theta(s_0 - t) \Big\{ & \frac{1}{\pi} Im\, \Psi^{KK}(t) \\ & + |B|^2 \frac{t^2}{288\,\pi^2} \left(\frac{f_K}{f_\pi}\right)^4 \int_{M_K^2}^{(\sqrt{t}-M_K)^2} dt_1 \int_{M_K^2}^{(\sqrt{t}-M_K)^2} dt_2\, 2\,\lambda^{3/2}(1, \tfrac{t_1}{t}, \tfrac{t_2}{t}) \\ & \qquad \times \frac{1}{\pi} Im\, \Pi_V^{(1)}(t_1) \frac{1}{\pi} Im\, \Pi_A^{(0)}(t_2) \Big\} \\ & + \Theta(t - s_0) \frac{1}{(16\pi^2)^3} \frac{2}{15} t^4 \{1 + \cdots\},\end{aligned} \tag{19}$$

where

$$\frac{1}{\pi} Im\, \Pi_A^{(0)}(t) = 2\, f_\pi^2\, \delta(t - M_K^2). \tag{20}$$

With this new *ansatz* for $\frac{1}{\pi} Im\, \Psi^{had}(t)$ we can then solve again for $|B|$. The new plots, to be compared with the previous ones, are also shown in Figs. 1 and 2 (the curves labeled (1)). In Fig. 1, curve (1), we show the new result when we only use the leading behaviour of $F(s_0)$, (A.7a); and in Fig. 2, curve (1), the result with the use of the full expression for $F(s_0)$ in (A.6a). We observe that the new minimum is lower than the previous one, and the corresponding s_0-value ($s_0 \approx 3.5$ GeV^2) is higher. The curve (1) in Fig. 2 shows roughly three regimes. An asymptotic regime for large s_0; a low-s_0 behaviour dominated by the $\frac{1}{s_0}$-power terms in $F(s_0)$; and an intermediate regime where an inflection point appears. The best determination we can suggest for $|B|$ from the simple *ansatz* in (19) is then the values delimited by the two extreme regimes at each side of the inflection point; *i.e.*,

$$0.75 \leq |\hat{B}| < 1 \tag{21}$$

Note that the positivity of the spectral function (5) implies that this rough estimate of $|B|$ is in fact an upper bound on the actual value of $|\hat{B}|$. The r.h.s.

of (6) is a sum of positive contributions from the different intermediate hadronic states, times a global factor proportional to $|B|^2$. The truncation to only a few intermediate states (K^0K^0 in (12); K^0K^0 and $KK\pi$ in (19)) obviously results in an underestimate of the hadronic spectral function and therefore in an overestimate of $|B|^2$ (the product is fixed by the QCD calculation of $F(s_0)$). This is nicely illustrated by Fig. 2: The inclusion of the $KK\pi$ intermediate state has resulted in B-values which are smaller than the ones obtained with only the KK contribution. The fact that B depends on the asymptotic freedom onset s_0, is just telling us that additional hadronic information is needed in order to balance the QCD information given by $F(s_0)$ (*i.e.*, to have duality between the QCD and hadronic parametrizations on both sides of (6)). The inclusion of additional intermediate states should result in a more stable prediction (less dependent on s_0), but always below the curves (0) and (1) in Fig. 2.

So far we have only used information based on the first Finite Energy Sum Rule in (6). It would be nice to have some further test of the "quality" of duality between QCD and the hadronic parametrizations which we are using as *ansatzs*, independently of the value of $|B|$ we want to determine. For this purpose, it was suggested in [1] to examine the dependence on s_0 of the ratio

$$<t_{eff}> = \frac{G(s_0)}{F(s_0)}\,; \tag{22}$$

i.e., the ratio of the first-moment (7) to the zeroth-moment (6), both as predicted by QCD and as a result of the various hadronic *ansatzs* in (6) and (7). For convenience, we choose to show plots of

$$\frac{6}{5\,s_0} <t_{eff}> \quad \text{versus} \quad s_0 \tag{23}$$

rather than $<t_{eff}>$ itself. The normalization factor $\frac{5\,s_0}{6}$ being precisely the value for $<t_{eff}>$ predicted by the leading behaviour due to asymptotic freedom; *i.e.*, in QCD

$$\lim_{s_0 \to \infty} \frac{6}{5\,s_0} <t_{eff}> = 1 + \mathcal{O}\left(\frac{\bar{\alpha}_s}{\pi}\right). \tag{24}$$

Figure 3 shows the plot in question. The line with the QCD label shows the prediction with α_s-corrections and the $\frac{1}{s_0}$-power corrections, discussed in the appendix, incorporated. It clearly approaches the asymptotic value (24) at large s_0-values. The hadronic parametrization correspondig to the K^0K^0-*ansatz* in (12) leads to the curve with the label (0). The improved parametrization proposed in (17)-(20) leads to the curve with the label (1). The overall duality picture is rather poor.

It is better, as expected, for the improved parametrization but not good enough. It is simply telling us that the tentative result in eq. (21) is not reliable.

We conclude from this analysis that to improve on the $|B|$ result in (21) requires further information on the hadronic spectral function. As we shall see in the next section, the 1^+ $K\pi\pi$ subchannel plays an important rôle in improving the duality picture and narrowing the error gap in the prediction of $|B|$. We shall discuss in the next section how to incorporate higher intermediate states beyond $\Gamma = K^0K^0$ and $\Gamma = KK\pi$; then, we shall come back in section 4 to the determination of the $|B|$-parameter.

We wish to conclude this section with an overview of the calculational approach we are proposing. Essentially, it consists in an effective hadronic realization of the four-quark operator $\mathcal{O}_{\Delta S=2}$ in (1) in terms of pseudoscalars, scalars, vector and axial-vector states. The effective chiral Lagrangian is only used to fix the threshold behaviours and the quantum number structure of possible resonant states. We insist that this is not a calculation like in chiral perturbation theory. If formulated in terms of an effective Lagrangian it would correspond rather to a tree level bosonic Lagrangian, which includes 0^-, 0^+, 1^- and 1^+ states, with an overall coupling constant that is the B-factor we want to determine.

This brings us to another question that some readers may ask: what is the possible effect of operators of higher dimension in the chiral realization? These operators are of two classes: operators with more than two derivatives and operators with more powers of quark masses. The first class should not be taken into account because they cannot contribute to the B-factor in (1) (each derivative requires one external field at least). Indeed we have not taken them into account. The second class however does contribute. Their effect is essentially a renormalization of the coupling constant B. In our approach, part of this effect is taken into account by the fact that we are using intermediate hadronic states with their physical masses and couplings. To do better than that would require a derivation from QCD of the tree level effective Lagrangian we mentioned above that is clearly beyond reach at present time.

3 PARAMETRIZATION OF HIGHER INTERMEDIATE STATES AND WEINBERG SUM RULES

As discussed in the previous section, the quantum numbers of the succesive intermediate states in the hadronic spectral function (5) can be read off from

the expansion in powers of Φ-fields in (10) and (15). The full hadronic spectral function in (5) appears then as a convolution of the sub-hadronic spectral functions modulated by the overall normalization factor $|B|^2$; *i.e.*,

$$\begin{aligned}
&\frac{1}{\pi}\,Im\,\Psi^{had}(t) = \\
&\Theta(s_0-t)\,|B|^2\frac{t^2}{288\,\pi^2}\left(\frac{f_K}{f_\pi}\right)^4\int_{t_{10}}^{(\sqrt{t}-\sqrt{t_{20}})^2}dt_1\int_{t_{20}}^{(\sqrt{t}-\sqrt{t_1})^2}dt_2\,\lambda^{1/2}(1,\tfrac{t_1}{t},\tfrac{t_2}{t}) \\
&\qquad\times\left\{\left(\tfrac{t_1}{t}+\tfrac{t_2}{t}-1\right)^2\frac{1}{\pi}\,Im\,\Pi^{(0)}(t_1)\,\frac{1}{\pi}\,Im\,\Pi^{(0)}(t_2)\right. \\
&\qquad+2\,\lambda(1,\tfrac{t_1}{t},\tfrac{t_2}{t})\,\frac{1}{\pi}\,Im\,\Pi^{(0)}(t_1)\,\frac{1}{\pi}\,Im\,\Pi^{(1)}(t_2) \\
&\qquad\left.+\left[\left(\tfrac{t_1}{t}+\tfrac{t_2}{t}-1\right)^2+8\,\tfrac{t_1}{t}\,\tfrac{t_2}{t}\right]\frac{1}{\pi}\,Im\,\Pi^{(1)}(t_1)\,\frac{1}{\pi}\,Im\,\Pi^{(1)}(t_2)\right\} \\
&+\Theta(t-s_0)\,\frac{1}{(16\,\pi^2)^3}\,\frac{2}{15}\,t^4\,\{1+\cdots\}.
\end{aligned} \tag{25}$$

Here the index $i = 0, 1$ in $\frac{1}{\pi}\,Im\,\Pi^{(i)}(t)$ refers to the angular momentum of the subspectral function in question; and for each $\frac{1}{\pi}\,Im\,\Pi^{(i)}(t)$ we have contributions from vector (V) and axial (A) channels; *i.e.*,

$$\frac{1}{\pi}\,Im\,\Pi^{(i)}(t) = \frac{1}{\pi}\,Im\,\Pi_V^{(i)}(t) + \frac{1}{\pi}\,Im\,\Pi_A^{(i)}(t). \tag{26}$$

We next proceed to the discussion of the parametrizations we propose for the various spectral functions .

3.1 The $\frac{1}{\pi}\,Im\,\Pi_A^{(0)}(t)$ spectral function

This corresponds to the channel with the quantum numbers of the K for which we take

$$\frac{1}{\pi}\,Im\,\Pi_A^{(0)}(t) = 2\,f_\pi^2\,\delta(t-M_K^2) + \Theta(t-t_0)\,\mathcal{O}\left(\frac{m_s^2}{t}\right), \tag{27}$$

where the second term represents the QCD asymptotic behaviour in this channel with $\bar{m}_s(t)$ the running strange quark mass. In practice, the effect of this term on the determination of the $|B|$-factor is negligible for $t_0 \geq 1$ GeV^2. With eq. (27) inserted in the r.h.s. of eq. (25) and upon integration , eq. (11) follows.

3.2 The $\frac{1}{\pi} Im\,\Pi_V^{(1)}(t)$ spectral function

This corresponds to the channel with the quantum numbers of the K^* which we have already discussed in (17), (18). In fact the $(L_\mu)_{23}$ matrix element in (15) has also a $K\eta$ contribution that is non-resonant and which we shall also include as part of the hadronic continuum. Therefore, the hadronic spectral function we propose for the 1^- channel is

$$\begin{aligned}\frac{1}{\pi} Im\,\Pi_V^{(1)}(t) \;=\; & \Theta(t_0 - t)\,\frac{1}{32\,\pi^2}\left\{\left(1 - \frac{M_K^2}{t}\right)^3 |f_{K^*}(t)|^2\,\Theta(t - M_K^2)\right. \\ & \left. + \lambda^{3/2}(1, \tfrac{M_K^2}{t}, \tfrac{M_\eta^2}{t})\,\Theta\,[t - (M_K + M_\eta)^2]\right\} \\ & + \Theta(t - t_0)\,\frac{1}{4\,\pi^2}\,\{1 + \cdots\},\end{aligned} \tag{28}$$

with the last term indicating the onset of the QCD asymptotic behaviour in this channel. We fix this continuum threshold t_0 by demanding that the integral

$$\int_{M_K^2}^{t_0} dt \frac{1}{\pi}\, Im\,\Pi_V^{(1)}(t)^{had} \;=\; \phi_V^{(1)}(t_0) \tag{29}$$

matches its QCD counterpart $\phi_V^{(1)}(t_0)$. The latter expression is given in (A.4) of the appendix. Numerically, we find

$$t_0(1^-) \;=\; 1.6\,\mathrm{GeV}^2. \tag{30}$$

3.3 The $\frac{1}{\pi} Im\,\Pi_V^{(0)}(t)$ spectral function

This corresponds to the channel with the quantum numbers of the $K_0^*(1430)$. The spectral function is proportional to the one associated to the divergence of the strangeness changing vector current, and therefore it vanishes in the limit $m_s \to 0$. Again, as in the 1^- case, it has a $K\pi$ which resonates as the $K_0^*(1430)$ and a $K\eta$ non resonant background. Following the same idea of using the chiral realization to predict the threshold behaviour and modulate the corresponding expressions with appropriate Breit-Wigner factors as in (18), we propose as a parametrization of this spectral function the expression

$$\begin{aligned}\frac{1}{\pi} Im\,\Pi_V^{(0)}(t) \;=\; & \Theta(t_0 - t)\,\frac{3}{32\,\pi^2}\left\{\left(\frac{M_K^2}{t}\right)^2\left(1 - \frac{M_K^2}{t}\right)|f_{K_0^*}(t)|^2\,\Theta(t - M_K^2)\right. \\ & \left. + \lambda^{1/2}(1, \tfrac{M_K^2}{t}, \tfrac{M_\eta^2}{t})\left(\frac{M_\eta^2 - M_K^2}{t}\right)^2\Theta\,[t - (M_K + M_\eta)^2]\right\} \\ & + \Theta(t - t_0)\mathcal{O}\left(\frac{m_s^2}{t}\right),\end{aligned} \tag{31}$$

where the last term represents the QCD asymptotic behaviour in this channel. It appears to be the same as the one of the 0^+ spectral function in (27) because the d-quark mass has been set to zero. For $t_0 \gtrsim 1$ GeV^2, the effect of the QCD continuum in (31) on the determination of $|B|$ is also negligible.

3.4 The $\frac{1}{\pi} Im\,\Pi_A^{(1)}(t)$ spectral function

This corresponds to the channel with the quantum numbers of the $K_1(1270)$. It is a rather complex channel which we must discuss in detail.

From the point of view of the chiral realization it is generated by the third term in the Φ-expansion of L_μ in (15); *i.e.*, it is a $K\pi\pi$ intermediate state. As with the other channels, the behaviour at threshold is unambigously predicted by the chiral spectral function. The complexity appears because now we have various possible resonant subchannels:

$K\ -\ \rho$	from the term	$[K, [\pi, \partial_\mu \pi]]$.
$K^*\ -\ \pi$	from the term	$[\pi, [K, \partial_\mu \pi]]$.
$K_0^*\ -\ \pi$	from the term	$[\pi, [K, \partial_\mu \pi]]$.

Each subchannel will be modulated by the appropriate Breit-Wigner factor. Furthermore, we have an overall resonant behaviour which we have to fix. This is where the difficulties appear because phenomenologically there exist two rather near K_1-states (in the notation of the Particle Data Group: the $K_1(1270)$ and the $K_1(1400)$). We propose three types of parametrizations and examine later how they satisfy the 1^{st} Weinberg Sum Rule for $S = 1$ spectral functions [12]. The three parametrizations we shall try are

a) Overall Breit-Wigner fit to the $K\pi\pi$ data [14]; *i.e.*,

$$|F^{(a)}(t)|^2 = \frac{1}{(t - M^2_{K\pi\pi})^2 + M^2_{K\pi\pi}\Gamma^2_{K\pi\pi}}. \tag{32}$$

b) Mixing of two complex poles adjusted to fit the $K\pi\pi$ data [14]; *i.e.*,

$$|F^{(b)}(t)|^2 = |F_1(t) + \xi\, F_2(t)|^2, \tag{33}$$

with

$$F_i(t) = \frac{1}{t - M_i^2 + i\, M_i\, \Gamma_i}, \tag{34}$$

and M_1, M_2, Γ_1, Γ_2 and complex ξ as free parameters.

c) Mixing of two complex poles.

$$|F^{(c)}(t)|^2 = |F_1(t) + \xi\, F_2(t)|^2 \tag{35}$$

with M_1, Γ_1, M_2 and Γ_2 fixed as in the Particle Data Booklet [13] and ξ a complex free parameter, that is used to fit the $K\pi\pi$ data [14].

It is understood that in each case the overall normalization is fixed so as to reproduce the chiral realization result at $t = 0$. Therefore, the hadronic spectral function we propose for the 1^+ channel is ($\alpha = a, b, c$):

$$\begin{aligned}
&\frac{1}{\pi}\, Im\, \Pi_A^{(1)}(t) = \frac{1}{(16\,\pi^2)^2}\frac{1}{6\, f_\pi^2}\frac{|F^{(\alpha)}(t)|^2}{|F^{(\alpha)}(0)|^2}\,\Theta(t - M_K^2)\,\Theta(t_0 - t) \\
&\times \left\{ \frac{1}{9}\int_0^{(\sqrt{t}-M_K)^2} dt_1\, \lambda^{1/2}(1, \tfrac{M_K^2}{t}, \tfrac{t_1}{t}) \left[1 + 10\,\tfrac{t_1}{t} - 2\,\tfrac{M_K^2}{t} + \left(\tfrac{t_1 - M_K^2}{t}\right)^2\right] |f_\rho(t_1)|^2 \right. \\
&+ \tfrac{1}{4}\int_{M_K^2}^{t} dt_1 \left(\tfrac{M_K^2}{t_1}\right)^2 \left(1 - \tfrac{M_K^2}{t_1}\right)\left(1 - \tfrac{t_1}{t}\right)^3 |f_{K_0^*}(t_1)|^2 \\
&\left. + \tfrac{1}{12}\int_{M_K^2}^{t} dt_1 \left(1 - \tfrac{M_K^2}{t_1}\right)^3 \left(1 - \tfrac{t_1}{t}\right)\left[1 + 10\,\tfrac{t_1}{t} + \left(\tfrac{t_1}{t}\right)^2\right] |f_{K^*}(t_1)|^2 \right\} \\
&+ \Theta(t - t_0)\,\tfrac{1}{4\,\pi^2}\{1 + \cdots\},
\end{aligned} \tag{36}$$

with the last term indicating the onset of the QCD asymptotic behaviour in this channel. As with the other spectral functions, this t_0 threshold is fixed by the QCD-hadronic duality constraint

$$\int_{M_K^2}^{t_0} dt\, \tfrac{1}{\pi}\, Im\, \Pi_A^{(1)}(t)^{had} = \phi_A^{(1)}(t_0), \tag{37}$$

where the QCD expression for $\phi_A^{(1)}(t_0)$ is given in (A.4) of the appendix.

The numerical values of the various parameters corresponding to the three parametrizations a), b) and c) above are:

Case a) : $M_{K\pi\pi} = 1.29$ GeV, $\Gamma_{K\pi\pi} = 0.215$ GeV.

$t_0 = 3.2$ GeV^2.

Case b) : $M_1 = 1.25$ GeV, $\Gamma_1 = 0.160$ GeV.

$M_2 = 1.39$ GeV, $\Gamma_2 = 0.180$ GeV.

$\xi = 0.29 + i\,0.65$.

$t_0 = 4.7$ GeV^2.

Case c) : $M_1 = 1.270$ GeV, $\Gamma_1 = 0.090$ GeV.

$M_2 = 1.402$ GeV, $\Gamma_2 = 0.174$ GeV.

$\xi = 1.25 + i\,0.60$.

$t_0 = 5.3$ GeV^2.

3.5 The 1st Weinberg Sum Rule (WSR)

This sum rule [12], when applied to $S = 1$ spectral functions implies that

$$\int_0^\infty dt\, Im\left(\Pi_V^{(1)}(t) + \Pi_V^{(0)}(t) - \Pi_A^{(1)}(t) - \Pi_A^{(0)}(t)\right) = 0. \tag{38}$$

The sum rule is a property of QCD in the chiral limit $m_s = m_d = m_u = 0$. It has been shown [15] that even in the presence of finite quark masses there is a 1st WSR of the type

$$\begin{aligned}
\int_0^{s_0} dt\, \tfrac{1}{\pi}\, Im\left(\Pi_V^{(1)} + \Pi_V^{(0)} - \Pi_A^{(1)} - \Pi_A^{(0)}\right)(t) &= \mathcal{O}\left(\tfrac{\bar{\alpha}_s}{\pi}\, m_s m_d\right) \\
&+ \mathcal{O}\left(\tfrac{m^4}{s_0}\log(s_0)\right) + \mathcal{O}\left(\tfrac{|<\bar{\Psi}\Psi>|^2}{s_0^2}\right).
\end{aligned} \tag{39}$$

The last term in the r.h.s. is the order expected from spontaneous chiral symmetry breaking [16]. This sum rule offers a powerful check of the consistency between the parametrizations we have proposed above. Figure 4 shows the dependence of the integral

$$WSR(s_0) \equiv \int_0^{s_0} dt\, \tfrac{1}{\pi}\, Im\left(\Pi_V^{(1)} + \Pi_V^{(0)} - \Pi_A^{(1)} - \Pi_A^{(0)}\right)(t) \tag{40}$$

on s_0 for the three parametrizations of $\frac{1}{\pi} Im\,\Pi_A^{(1)}(t)$ which we have discussed above. They correspond to the curves a), b) and c) in the Figure. We conclude from this that the three parametrizations fulfil the 1^{st} WSR in a similar way. We choose the parametrization c) as the more realistic one since two resonant states, $K_1(1270)$ and $K_1(1400)$, have been reported experimentally [13]. We shall use the other two parametrizations as an indication of the error induced by the hadronic parametrization of this channel.

4 DETERMINATION OF THE $|B|$-FACTOR

We now wish to see how the curves (0) and (1) in Figures 1 and 2 change as we go on adding more hadronic input. We recall that curves (0) in these figures correspond to the lowest hadronic state K^0K^0 and curves (1) to the sum $K^0K^0 + KK\pi$. The other curves in Figures 1 and 2 correspond to the results we find when we go on adding one more state with one more pion in the hadronic spectral function of (25); *i.e.*, the various curves correspond to the following physical content:

Curve	Intermediate states	Resonances
(0)	K^0K^0	
(1)	$K^0K^0 + KK\pi$	K^*
(2)	$K^0K^0 + KK\pi + KK2\pi$	$K^*, 2K^*, K_1$
(3)	$K^0K^0 + KK\pi + KK2\pi + KK3\pi$	K^* , $2K^*$, K_1 , K_1 K^*
(4)	$K^0K^0 + KK\pi + KK2\pi + KK3\pi$ $+KK4\pi$	K^* , $2K^*$, K_1 , K_1 K^* , $2K_1$
(5)	$K^0K^0 + KK\pi + KK2\pi + KK3\pi$ $+KK4\pi$ + continuum	K^* , $2K^*$, K_1 , K_1 K^* , $2K_1$

The last column indicates the content in $J = 1$ resonant states. In Fig. 1 we clearly see a displacement of the minimum towards higher values of s_0 and lower values of $|B|$. The shape of the minimum is also wider indicating better and better stability as we go on from curve (0) to curve (5). These are the results when we only use the leading behaviour of $F(s_0)$ in (A.7a). Since the corrections to this behaviour are negative, we can view the succesive minima as succesive upper bounds for $|B|$.

Next we want to see the corresponding evolution of the plots with the full expression for $F(s_0)$ as given in (A.6a) which are also strict upper bounds for $|B|$. This we show in Figure 2. The previous minimum becomes now an inflection point

that is also displaced towards smaller values of $|B|$ and larger-s_0 values as we go from the curve (0) to the curve (5). At these rather large-s_0 values $s_0 \geq 6$ GeV^2 the QCD corrections in the functions $F(s_0)$ and $G(s_0)$ are already moderate.

The last thing we want to examine is the test of "quality" of duality between QCD and the hadronic parametrizations; *i.e.*, the plot of

$$\frac{6}{5\,s_0} < t_{eff} > \quad \text{versus} \quad s_0 \tag{41}$$

with $< t_{eff} >$ defined in (22). Figure 3 shows this plot for the succesive parametrizations (0), (1), $\cdots$, (5). We clearly see an improvement in the hadronic-QCD duality as we go on introducing more and more states.

Our best estimate of $|B|$ follows from curve (5) in which we have included all the intermediate thresholds. It is also the one showing the best stability and the best duality. The inflection point occurs at $s_0 = 6.8$ GeV^2 and corresponds to a $|\hat{B}| \approx 0.39$. On the other hand the duality region between 6 GeV^2 and 10 GeV^2 is rather good. We suggest to take the $|B|$-values at these extreme points as an indication of part of the error on the central value fixed at the inflection point. To this we add a further error that includes the range of the values for the B-factor obtained by using the other two hadronic parametrizations for the axial-vector channel; *i.e.*; the parametrizations a) and b) given in section 3.4. With this criterion we are led to the final result

$$|\hat{B}| = 0.39 \pm 0.10. \tag{42}$$

The error here, however, does not include possible systematic errors of the method of approximations we are using. (See the discussion at the end of section 2.)

The result above is compatible with the one found in [1]; *i.e.*, eq. (3). It is also compatible with the current algebra calculation of [9] and some of the QCD sum rules calculations based on three-points functions [2],[4]. It is lower than the values reported by the authors of [5] based on their $N_c \to \infty$ limit approach but it is compatible with the recent results of [17] based on an approximate calculation, also within the $\frac{1}{N_c}$-expansion framework, of the QCD effective action of the $\mathcal{O}_{\Delta S=2}$-operator. It disagrees with the published results based on lattice gauge simulations reported by three independent groups [6], [7] and [8] which give higher values (see however ref. [18]).

ACKNOWLEDGEMENTS

We are grateful to N.Bilić and B.Guberina for discussions and for their collaboration in the early stages of this work. J.P. and E. de R. would like to thank the CERN theory group for its hospitality. C.D. acknowledges support from the FRD (South Africa). The work of three of us, J.A.P., A.P. and J.P., has been supported in part by CICYT (Spain) under grant No. AEN90-0040. Finally, J.P. is also indebted to the Spanish Ministerio de Educación y Ciencia for a fellowship.

APPENDIX

This section collects the expressions corresponding to the QCD counterparts of the Finite Energy Sum Rules (FESR) that appear along the text. We also give the values of the input parameters used in our calculations.

A.1 Sum Rules for current correlators

Given a current $J(x)$ with definite quantum numbers we can construct the following correlation function

$$\Pi_J(q) \equiv i \int d^4x e^{iqx} <0|T(J(x)J^\dagger(0))|0>. \tag{A.1}$$

The analyticity of $\Pi_J(q)$ allows us to establish a duality relation which reads as follows

$$\int_{th}^{t_0} dt \frac{1}{\pi} Im\, \Pi_J^{had}(t) = -\frac{1}{2\pi i} \oint_{C_{t_0}} dt\, \Pi_J^{QCD}(t) \equiv \phi_J(t_0). \tag{A.2}$$

This is the so-called zeroth momentum FESR.

The spectral function with $\Delta S = 2$ (25) involves intermediate states with quantum numbers $J^P = 0^-$, 0^+, 1^- and 1^+. We have parametrized the spectral functions corresponding to these intermediate states in the following way,

$$\frac{1}{\pi} Im\, \Pi_J^{had}(t) = \Theta(t_0 - t) \frac{1}{\pi} Im\, \Pi_J^{ef\!f}(t) + \Theta(t - t_0) \frac{1}{\pi} Im\, \Pi_J^{QCD}(t). \tag{A.3}$$

The expressions for the spectral functions (A.3) that correspond to the states K, K_0^*, K^* and K_1 are given in the text by (27), (28), (31) and (36), respectively.

We have set the value for the QCD continuum onset, t_0, in the $J = 1$ channels by requiring the fulfilling of (A.2) for each spectral function mentioned above (equ. (29) and (37)).

The QCD counterpart $\phi_J(t_0)$ for these current correlators are given by (we consider the down quark as massless),

$$\phi_V^{(1)}(t_0) = \phi_A^{(1)}(t_0) = \frac{t_0}{4\pi^2} \left(1 + \frac{\bar{\alpha}_s}{\pi}(t_0) + F_3 \left(\frac{\bar{\alpha}_s}{\pi}(t_0)\right)^2 + \mathcal{O}\left(\left(\frac{\bar{\alpha}_s}{\pi}\right)^3\right)\right), \tag{A.4}$$

$$\phi_V^{(0)}(t_0) = \phi_A^{(0)}(t_0) = \mathcal{O}\left(\frac{m_s^2}{t_0}\right) \approx 0, \tag{A.5}$$

with $F_3 = 1.986 - 0.115\, n_F$, and $n_F = 3$ (number of effective flavours).

A.2 Sum Rules for the two-point function with $\Delta S = 2$, $\Psi(q^2)$.

The QCD realization for the two functions $F(s_0)$ and $G(s_0)$ that appear in (6) and (7), respectively, has been evaluated within perturbative QCD and including the power corrections *à la* Shifman, Vainshtein and Zakharov (SVZ) [11] parametrized by the condensates $m_s<\bar{s}s>$ and $<\frac{\alpha_s}{\pi}G^2>$. The explicit form for $F(s_0)$ and $G(s_0)$ is given by [1]

$$\begin{aligned} F(s_0) = \frac{1}{(16\pi^2)^3} \left[\frac{\alpha_s'''(\mu^2)}{\alpha_s'''(s_0)}\right]^{4/9} \frac{2 s_0^5}{75} \Bigg[1 - \frac{1379}{810} \frac{\bar{\alpha}_s}{\pi}'''(s_0) + \mathcal{O}\left(\left(\frac{\bar{\alpha}_s}{\pi}\right)^2\right) \\ - 50 \frac{\bar{m}_s^2(s_0)}{s_0} - \frac{5}{3} \frac{<\Omega>}{s_0^2} + \mathcal{O}\left(\frac{<\mathcal{O}_6>}{s_0^3}\right)\Bigg], \end{aligned} \tag{A.6a}$$

$$\begin{aligned} G(s_0) = \frac{1}{(16\pi^2)^3} \left[\frac{\alpha_s'''(\mu^2)}{\alpha_s'''(s_0)}\right]^{4/9} \frac{s_0^6}{45} \Bigg[1 - \frac{1352}{810} \frac{\bar{\alpha}_s}{\pi}'''(s_0) + \mathcal{O}\left(\left(\frac{\bar{\alpha}_s}{\pi}\right)^2\right) \\ - 48 \frac{\bar{m}_s^2(s_0)}{s_0} - \frac{3}{2} \frac{<\Omega>}{s_0^2} + \mathcal{O}\left(\frac{<\mathcal{O}_6>}{s_0^3}\right)\Bigg], \end{aligned} \tag{A.6b}$$

where $<\Omega> \equiv 200 \bar{m}_s^4(s_0) - 20\pi^2[16 m_s <\bar{s}s> - <\frac{\alpha_s}{\pi}G^2>]$.

The leading behaviour of these functions at large s_0 is

$$F(s_0) = \frac{1}{(16\pi^2)^3} \left[\frac{\alpha_s'''(\mu^2)}{\alpha_s'''(s_0)}\right]^{4/9} \frac{2 s_0^5}{75}, \tag{A.7a}$$

$$G(s_0) = \frac{1}{(16\pi^2)^3} \left[\frac{\alpha_s'''(\mu^2)}{\alpha_s'''(s_0)}\right]^{4/9} \frac{s_0^6}{45}. \tag{A.7b}$$

The anomalous dimension of the operator $\mathcal{O}_{\Delta S=2}(x)$ turns out in the scale dependence of the $\alpha_s^{'''}(\mu^2)^{4/9}$ factor that appears both in $F(s_0)$ and $G(s_0)$. The running coupling $\bar{\alpha}_s^{'''}$ and running mass $\bar{m}_s$ are supposed to be computed in an effective theory with only three light quark flavours in the $\overline{\rm MS}$ renormalization scheme.

In the text it is also proposed the study of the following ratio

$$<t_{eff}> \equiv \frac{G(s_0)}{F(s_0)} \tag{A.8}$$

as a test of duality for the hadronic parametrization of $\frac{1}{\pi} Im\, \Psi(q^2)$. The QCD asymptotic behaviour of $\frac{6}{5s_0}<t_{eff}>$ is given by the expression

$$\begin{aligned}\frac{6}{5s_0}<t_{eff}> = 1 + \frac{1}{30}\frac{\bar{\alpha}_s}{\pi}^{'''}(s_0) + \frac{2\bar{m}_s^2(s_0)}{s_0} + \frac{1}{6}\frac{<\Omega>}{s_0^2} \\ + \frac{100\,\bar{m}_s^4(s_0)}{s_0^2} + \mathcal{O}\left(\left(\frac{\alpha_s}{\pi}\right)^2\right) + \mathcal{O}\left(\frac{<\mathcal{O}_6>}{s_0^3}\right).\end{aligned} \tag{A.9}$$

A.3 Parameters and formulae used

The running quark mass $\bar{m}_s(t)$ is given by

$$\bar{m}_s(t) = \hat{m}_s\left(\frac{9}{2}\frac{\bar{\alpha}_s}{\pi}(t)\right)^{4/9}\left[1 + 0.89\frac{\bar{\alpha}_s}{\pi}(t) + 1.37\left(\frac{\bar{\alpha}_s}{\pi}(t)\right)^2\right]. \tag{A.10}$$

We have used the value $\hat{m}_s = 288 \pm 48$ MeV [19] for the invariant strange quark mass, and $\Lambda_{QCD} = 100 - 200$ MeV. The value of the strange quark condensate we use is $m_s<\bar{s}s> = -2.34 \times 10^{-3}$ GeV^4. For the gluon condensate we have taken the range $<\frac{\alpha_s}{\pi}G^2> = (1.2 - 2.4) \times 10^{-2}$ GeV^4.

The result of these variations on the B-factor is contained in the error we have stated in (42).

References

[1] A. Pich and E. de Rafael, Phys. Lett. **158 B** (1985) 477.

[2] N. Bilić, C.A. Dominguez and B. Guberina, Z. Phys. **C 39** (1988) 351.

[3] K.G. Chetyrkin, A.L. Kataev, A.B. Krasulin and A.A. Pivovarov, Phys. Lett. **B 174** (1986) 104.

[4] R. Decker, Nucl Phys. **B 277** (1986) 661.

[5] W.A. Bardeen, A.J. Buras and J.-M. Gérard, Phys. Lett. **B 193** (1987) 138, ibid. **B 211** (1988) 343.

[6] M.B. Gavela, L. Maiani, S. Petrarca, F. Rapuano, G. Martinelli, O. Pène and C.T. Sachrajda, Nucl. Phys. **B 306** (1988) 677.

[7] C. Bernard, T. Drapper, G. Hockney and A. Soni, Nucl. Phys. **B** (Proc. Suppl.) 4 (1988) 483.

[8] G. Kilcup, S.R. Sharpe, R. Gupta and A. Patel, Phys. Rev. Lett. **D 64** (1990) 25.

[9] J.F. Donoghue, E. Golowich and B.R. Holstein, Phys. Lett. **119 B** (1982) 412.

[10] R.A. Bertlmann, G. Launer and E. de Rafael, Nucl. Phys. **B 250** (1985) 61.

[11] M.A. Shifman, A.I. Vainshtein and V.I. Zakharov, Nucl. Phys. **B 147** (1979) 385.

[12] S. Weinberg, Phys. Rev. Lett. **18** (1967) 507.

[13] Particle Data Group, Phys. Lett. **B 239** (1990) 1.

[14] C. Daum et al., Nucl. Phys. **B 187** (1981) 1.

[15] E. Floratos, S. Narison and E. de Rafael, Nucl. Phys. **B 155** (1979) 115.

[16] P. Pascual and E. de Rafael, Z. Phys. **C 12** (1982) 127.

[17] A. Pich and E. de Rafael, preprint CERN-TH.5906/90; CPT-90/P.2393.

[18] S.R. Sharpe, Contribution to the International Symposium "Lattice '90" (Tallahasee, Florida, 8-12 October 1990), NSF-ITP-90-204.

[19] E. de Rafael and C.A. Dominguez, Ann. Phys. **174** (1987) 372.

FIGURE CAPTIONS

1) Curves showing the s_0 dependence of the $\hat{B}$-factor obtained by using the leading behaviour of QCD, eq. (A.7a), and with the inclusion of the following intermediate hadronic states: K^0K^0 in curve (0); $K^0K^0 + KK\pi$ in curve (1); $K^0K^0 + KK\pi + KK2\pi$ in curve (2); $K^0K^0 + KK\pi + KK2\pi + KK3\pi$ in curve (3); $K^0K^0 + KK\pi + KK2\pi + KK3\pi + KK4\pi$ in curve (4); the curve (5) has the same hadronic content as curve (4) with the addition of the QCD continuum.

2) This figure shows the same curves as in Fig. 1 but including the full expression for QCD, eq. (A.6a).

3) These curves show the s_0 dependence of the quantity $\frac{6<t_{eff}>}{5s_0}$, eq. (24). The higher curve is the QCD prediction, eq. (A.9). The labels (0), $\cdots$ (5) have the same explanation given in Fig. 1.

4) Here we plot the 1st WSR for the channel with S = 1, eq. (40), corresponding to the three hadronic parametrizations for the axial-vector channel a), b) and c) given in section 3.4.

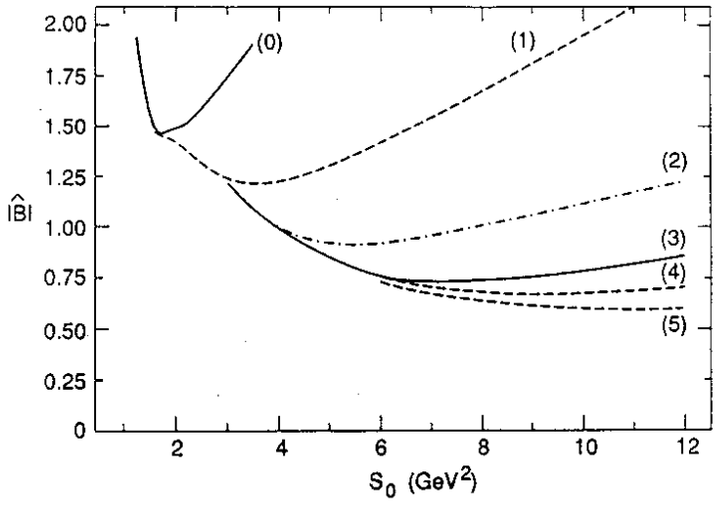

- Figure 1 -

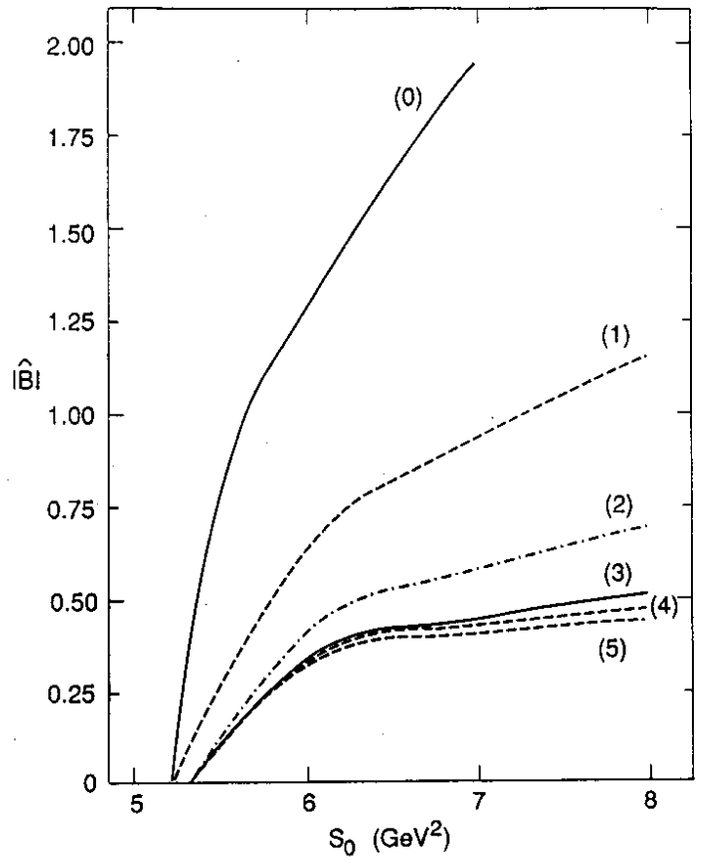

- Figure 2 -

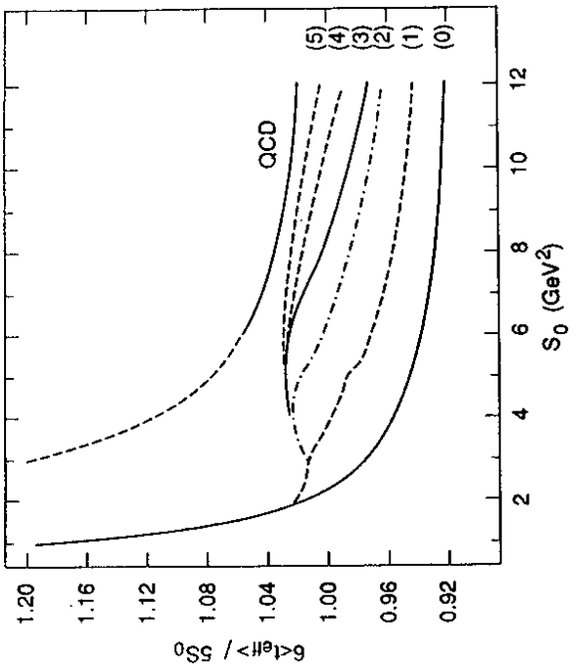

- Figure 3 -

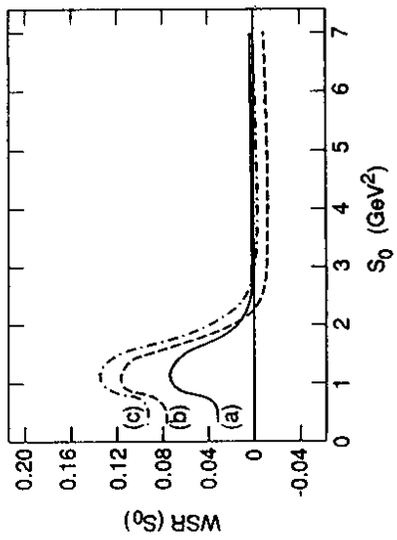

- Figure 4 -

Imprimé au CERN. Prix : 0.35 Fr.